

# Differentiating the Higgs boson from the dilaton and the radion at hadron colliders

Vernon Barger, Muneyuki Ishida<sup>†</sup>, and Wai-Yee Keung<sup>‡</sup>

*Department of Physics, University of Wisconsin, Madison, WI 53706, USA*

<sup>†</sup> *Department of Physics, Meisei University, Hino, Tokyo 191-8506, Japan*

<sup>‡</sup> *Department of Physics, University of Illinois, Chicago, IL 60607, USA*

(Dated: March 7, 2012)

## Abstract

A number of candidate theories beyond the standard model (SM) predict new scalar bosons below the TeV region. Among these, the radion, which is predicted in the Randall-Sundrum model, and the dilaton, which is predicted by the walking technicolor theory, have very similar couplings to those of the SM Higgs boson, and it is very difficult to differentiate these three spin-0 particles in the expected signals of the Higgs boson at the LHC and Tevatron. We demonstrate that the observation of the ratio  $\sigma(\gamma\gamma)/\sigma(WW)$  gives a simple and decisive way, independently of the values of model parameters: the VEVs of the radion and dilaton fields.

A number of candidate theories beyond the Standard Model (SM) predict new scalar bosons below the TeV region. When a scalar boson signal is detected in the Higgs search at the LHC, it is very important to determine whether it is really a SM Higgs boson or another exotic scalar. Among these, the radion( $R$ ), predicted in the Randall-Sundrum (RS) model[1–18], and the dilaton( $D$ ), predicted in spontaneous *scale symmetry* breaking[19–25], have very similar couplings to those of the standard model Higgs boson ( $H$ ), and it is very difficult to differentiate these three particles,  $DHR$ , in the signals. A distinctive difference[17, 19, 26, 27] is in their couplings to massless gauge bosons. We demonstrate that the ratios  $\sigma(\gamma\gamma)/\sigma(WW)$  are different from each other, and their observation gives a decisive method to distinguish these three spin-0 particles. Our main result is given in Fig. 2. It is important that the  $\sigma(\gamma\gamma)/\sigma(WW)$  ratio is independent of the model-parameters; the VEVs of the radion and dilaton fields. The test applies to both LHC and Tevatron experimental searches.

For definiteness we consider the dilaton coupling given in ref.[19], which is the same as the dilaton coupling in 4-dimensional walking technicolor theory[21–25] where all SM fields are composites of strongly interacting fields in conformal field theory (CFT). In AdS/CFT correspondence this dilaton is dual to the radion[2–4] in the original Randall-Sundrum (RS1) model[1], where all the SM fields are localized at the infrared (IR) brane in the 5-dimensional Anti-de Sitter(AdS) space background. We consider the radion coupling of the Randall-Sundrum (RS2) model given in ref.[5] where all the SM fields are in the bulk[6–18]. The radion has bulk couplings to the gauge bosons. It is dual[5] to the dilaton in CFT. We do not consider flavor changing neutral current (FCNC) processes; however, we note that a dilaton in a particular CFT with SM fields that are elementary and weakly coupled can generically have FCNC[28, 29], as can the radion of the RS2 model[30] considered here. We will study collider signatures from the gauge coupling differences of  $DHR$  in the following.

*Effective Lagrangians* We treat the SM Higgs boson  $H$ , the radion  $R$ , and the dilaton  $D$ , which are also denoted as  $(\varphi^i) = (\varphi^1, \varphi^2, \varphi^3) = (h^0, \phi, \chi) \equiv (H, R, D)$ . The vacuum expectation values (VEV) of these fields are denoted as

$$(\mathcal{F}_i) = (F_1, F_2, F_3) = (-v, \Lambda_\phi, f) \quad (1)$$

for  $H$ ,  $R$ , and  $D$ , respectively. The  $F_i^{-1}$  determine overall coupling strengths of these particles, and  $F_1 = -v = -246$  GeV.

The Lagrangian  $L_{\text{eff}}$  of the interactions[3–5, 14, 16, 19] with the SM particles is given by

$$L_{\text{eff}} = L_A + L_V + L_f + L_h + L_{AV} \quad (2)$$

$$L_A = -\frac{\varphi^i}{4F_i} \left[ \left( \frac{1}{kL} + \frac{\alpha_s}{2\pi} b_{QCD}^i \right) \sum_a F_{\mu\nu}^a F^{a\mu\nu} + \left( \frac{1}{kL} + \frac{\alpha}{2\pi} b_{EM}^i \right) F_{\mu\nu} F^{\mu\nu} \right] \quad (3)$$

$$L_V = -\frac{2\varphi^i}{F_i} \left[ \left( m_W^2 W_\mu^+ W^{-\mu} + \frac{1}{4kL} W_{\mu\nu}^+ W^{-\mu\nu} \right) + \left( \frac{m_Z^2}{2} Z_\mu Z^\mu + \frac{1}{8kL} Z_{\mu\nu} Z^{\mu\nu} \right) \right] \quad (4)$$

$$L_{AV} = -\frac{\varphi^i}{F_i} \frac{\alpha}{4\pi} b_{Z\gamma}^i F_{\mu\nu} Z^{\mu\nu} \quad (5)$$

$$L_f = \frac{\varphi^i}{F_i} \sum_f I_f^i m_f \bar{f} f \quad (6)$$

$$L_h = \frac{\varphi^i}{F_i} (2m_h^2 h^2 - \partial_\mu h \partial^\mu h) \quad (7)$$

where  $L$  denotes the separation of the branes in the RS2 model and  $kL$  is a parameter that governs the weak scale-Planck scale hierarchy. The  $1/kL$  term is absent for the dilaton and the Higgs boson.  $L_A$  specifies the couplings to the massless gauge bosons, and  $F_{\mu\nu}^a(F_{\mu\nu})$  represents the field strength of gluon(photon).  $L_V$  gives the couplings to the weak bosons, and  $W_{\mu\nu}^+ = \partial_\mu W_\nu^+ - \partial_\nu W_\mu^+$  etc. In the fermion-coupling Lagrangian  $L_f$ , the factors are  $I_f^H = -1$  and  $I_f^D = 1$  for all fermions  $f$ , while the  $I_f^R$  depend upon the bulk wave functions of the fermion  $f$  in the RS2 model. We take  $I_b^R = 1.66$  for one value of  $b\bar{b}$  coupling[15] as our example.  $L_h$  represents the couplings to the Higgs boson.  $L_h$  is also applicable to the  $\varphi^i = R, D$ . In the radion effective interaction, the brane kinetic terms are taken to be zero[16].

A distinction in Eq. (3) is the  $gg$  and  $\gamma\gamma$  couplings  $\frac{1}{kL} + \frac{\alpha_{s,EM}}{2\pi} b_{QCD,EM}^i$ . Their expressions are given in Table I.  $b_{QCD,EM}^i$  is given by the sum of the triangle-loop contributions of top quark and  $W$  boson and the  $\beta$  function coefficient appearing in the trace-anomaly of the SM energy-momentum tensor  $T_{\mu\nu}(SM)$ [2, 4, 19, 25]. The trace-anomaly term contributes for  $R$  and  $D$  but not for  $H$ . Here we should note that the  $\beta$  function contributions (the second column) always count all favors "light or heavy". But, the mass-coupling-term of the triangle-loop diagram operates in a way to cancel the heavy countings if the  $D$  (or  $R$ ) masses are lower than the corresponding threshold. As a result,  $b_{QCD}^{R,D} = 11 - \frac{2}{3}5$  for  $m < 2m_t$  with the number of effective flavors  $n_f = 5$ . A similar argument is also applicable to  $b_{EM}^{R,D}$ .

The real part of the  $\gamma\gamma$  couplings are given in Fig. 1. The destructive interference between the bulk coupling term  $1/kL$  and the  $b_{EM}^R$  term is due to the opposite sign, and this yields

$R$	$D, R$	$D, R, H$
$\frac{1}{kL}$	$+\frac{\alpha_s}{2\pi}(11 - \frac{2}{3}6)$	$+\frac{\alpha_s}{2\pi}F_t$ ; $F_t = \begin{cases} \frac{2}{3} & m < 2m_t \\ 0 & 2m_t < m \end{cases}$
$\frac{1}{kL}$	$+\frac{\alpha}{2\pi}(\frac{19}{6} - \frac{41}{6})$	$+\frac{\alpha}{2\pi}(\frac{8}{3}F_t - F_W)$ ; $\frac{8}{3}F_t - F_W = \begin{cases} -\frac{47}{9} & m < 2m_W \\ -\frac{2}{9} & 2m_W < m < 2m_t \\ -2 & 2m_t < m \end{cases}$

TABLE I.  $gg$  and  $\gamma\gamma$  couplings,  $\frac{1}{kL} + \frac{\alpha_s}{2\pi}b_{QCD}^i$ (2nd row) and  $\frac{1}{kL} + \frac{\alpha}{2\pi}b_{EM}^i$ (3rd row), of  $DHR$  scalars: Only the third column contributes for  $H$  where  $F_t(F_W)$  represent the triangle-loop contributions of top quark and  $W$  boson which are given in ref.[31, 32, 34]. For  $D$ , both second and third columns contribute where the second column represents the trace-anomaly. For  $R$  the first column ( $1/kL$ ) also contributes. It comes from the bulk field coupling, The volume of the 5th dimension is taken to be  $kL = 35$  in  $R$ , while we can represent  $D, H$  with  $(1/kL) \rightarrow 0$ .

the very different shape of  $\sigma(\gamma\gamma)/\sigma(WW)$  versus  $m$ : The cusp at  $m = 2m_W$ , which comes from the  $WW$  threshold effect, constructively contributes for  $D$  and  $H$ , and destructively for  $R$ . This behavior is seen in Fig. 2.

$L_{AV}$  describes the  $Z\gamma$  decays. The effective couplings  $b_{Z\gamma}^i$  are given by

$$b_{Z\gamma}^i = -A_W - A_F + \frac{b_{Z\gamma}}{\sin\theta_W \cos\theta_W}, \quad b_{Z\gamma} = \frac{19}{6} + \frac{11}{3}\sin^2\theta_W \quad (8)$$

where  $R, H, D$  have both  $A_W$  and  $A_F$  terms from the triangle-loop contributions of  $W$  and SM fermions, respectively. Their explicit forms are given in refs.[31, 32].  $A_F$  is negligible compared to  $A_W$ . The third term comes from the trace anomaly of  $T_\mu^\mu(SM)$  and it contributes to  $R, D$ , but not to  $H$ . We can check that particles with heavier thresholds than  $m_D$  or  $m_R$  decouple also in  $Z\gamma$ . To a good approximation the bulk-field coupling of  $R$  gives no contribution to  $Z\gamma$ [33].

$\sigma(\gamma\gamma)/\sigma(WW)$  ratio From  $L_{\text{eff}}$  in Eq. (2), we can calculate the partial widths  $\Gamma$  of  $H, R$ , and  $D$ . They are proportional to the inverse squares of the overall constants  $F_i$ , but the values of  $F_R$  and  $F_D$  are presently unknown. However, the  $\sigma(\gamma\gamma)/\sigma(WW)$  ratios[34] are independent of these VEVs. Figure 2 shows the ratios  $\Gamma(\gamma\gamma)/\Gamma(WW) = \sigma(\gamma\gamma)/\sigma(WW)$  (upper figure), the ratios  $\Gamma(b\bar{b})/\Gamma(WW) = \sigma(b\bar{b})/\sigma(WW)$  (middle figure), and the ratios  $\Gamma(Z\gamma)/\Gamma(WW) = \sigma(Z\gamma)/\sigma(WW)$  (lower figure), for  $R$  and  $D$  of the same mass. They are compared with those of  $H$  of the same mass.

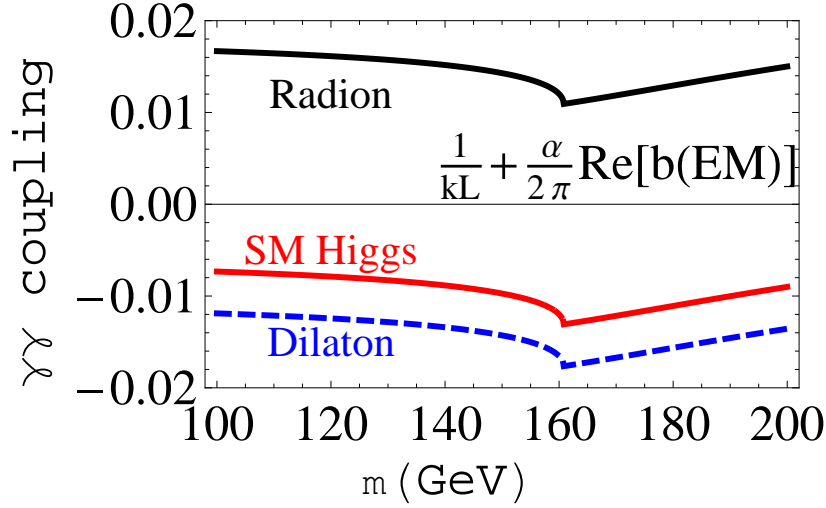


FIG. 1. The real part of the  $\gamma\gamma$  couplings,  $\frac{1}{kL} + \frac{\alpha}{2\pi} b_{EM}^i$  for  $i = H, D$ , and  $R$ . The bulk coupling term is given by  $kL = 35$  for  $R$ , while  $(1/kL) \rightarrow 0$  for  $D$  and  $H$ . The  $D$  has an additional contribution  $-\frac{11}{3}$  in  $b_{EM}^D$  compared to  $b_{EM}^H$ . The  $R$  has a contribution from the bulk field coupling which destructively interfere with the term of  $b_{EM}^R = b_{EM}^D$ . The imaginary parts contribute above the  $m > 2m_W$  and they only give subleading contributions.

As can be clearly seen in Fig. 2, we can differentiate the three scalars,  $R, D, H$ , by observing the ratio  $\sigma(\gamma\gamma)/\sigma(WW)$ . In Fig. 2 the slope changes around  $m \simeq 2m_W$  since  $\Gamma(WW)$  steeply decreases below the  $WW$  threshold. The  $R$  gives an almost constant ratio in  $m_R > 2m_W$  because of the contribution from the bulk coupling term  $1/kL$  which is energy-independent. The drastic change in slope of the ratio of  $R$  near  $m \simeq 2m_W$  occurs from the interference between this bulk coupling and the trace anomaly term. See, Fig. 1.

The ratio  $\sigma(b\bar{b})/\sigma(WW)$  of  $R$  can differ from  $H$  and  $D$ , because of the parameter  $I_b^R$ , so measuring this quantity is also helpful to distinguish  $R$  from the other two scalars.

The ratio  $\sigma(Z\gamma)/\sigma(WW)$  of  $R$  and  $D$  can differ from  $H$ , because of the trace anomaly contributions. This channel is helpful to determine the coupling form of the signal. It may be possible to detect it by focusing on the monochromatic photon spectrum from  $H \rightarrow Z\gamma$ .

#### Total widths and decay branching fractions (BF)

The total widths of  $R, D, H$  are given in Fig. 3.  $\Gamma_{\text{tot}}^R(\Gamma_{\text{tot}}^D)$  scale with  $(v/F_R)^2$  ( $(v/F_D)^2$ ) where  $F_R = F_D = 3$  TeV are taken, and the  $R$  and  $D$  widths are about two orders of

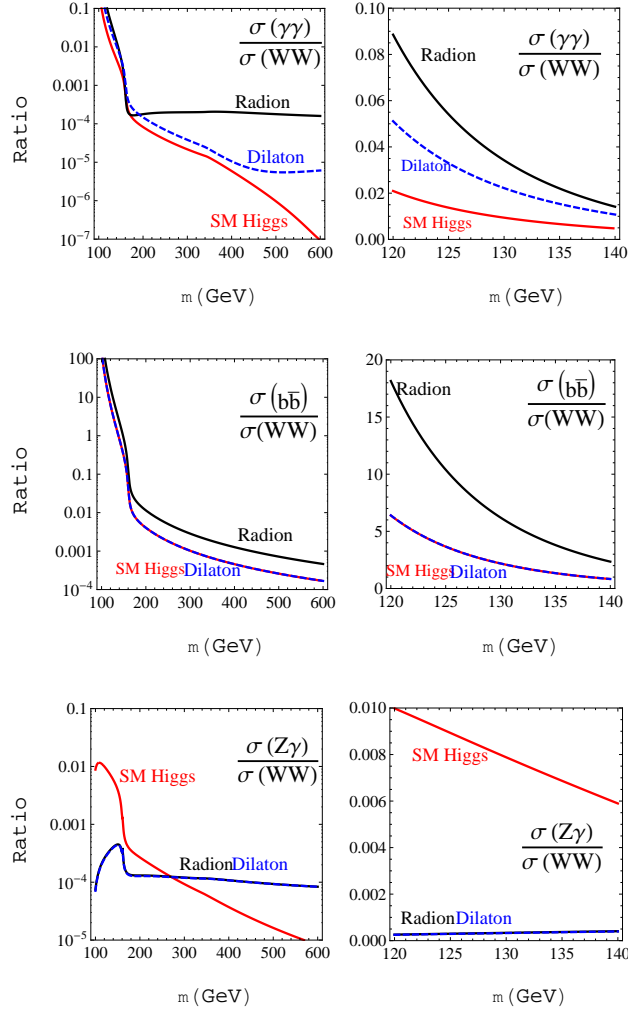


FIG. 2. The cross section ratios,  $\sigma(\gamma\gamma)/\sigma(WW)$  and  $\sigma(b\bar{b})/\sigma(WW)$  versus the mass of the scalar:  $H, R, D$ . For the radion (black solid), the dilaton (blue dashed), and the SM Higgs (red dotted) for  $\sigma(\gamma\gamma, b\bar{b}, Z\gamma)/\sigma(WW)$  (upper, middle, lower figures). The ratios are independent of the values of the model parameters,  $F_R$  and  $F_D$ .  $H$  and  $D$  have the same value of  $\sigma(b\bar{b})/\sigma(WW)$  while for  $R$  it can be different, since the ratio is proportional to the square of the parameter  $I_b^R$  that is taken to be 1.66 as an example.  $\sigma(Z\gamma)/\sigma(WW)$  of  $R$  and  $D$  are different from that of  $H$  due to the trace-anomaly contribution.

magnitudes smaller than the  $\Gamma_{\text{tot}}^H$  with the same mass.

The branching fractions ( $BF$ ) of the decays to  $\bar{X}X = WW, \gamma\gamma, b\bar{b}, gg, Z\gamma$  are compared in Fig. 4, where the  $K$ -factor in NNLO[35] is considered for  $gg$ .  $BF(\gamma\gamma)$  shows very delicate

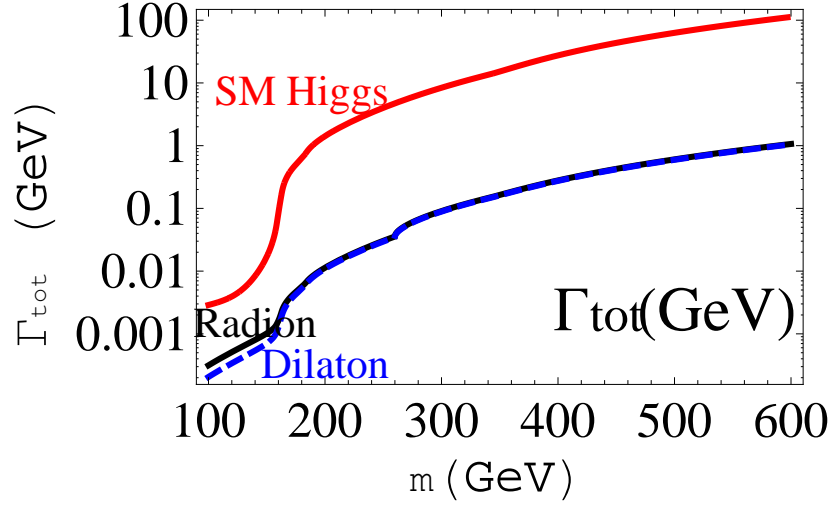


FIG. 3. The total widths (GeV) of the radion  $R$  (black solid), dilaton  $D$  (blue dashed), and SM Higgs  $H$  (red dotted).  $\Gamma_{\text{tot}}^R, \Gamma_{\text{tot}}^D$  scale with  $(v/F_R)^2, (v/F_D)^2$ , respectively, where  $F_R$  and  $F_D$  are commonly taken to be 3 TeV.

structures.  $BF(H \rightarrow \gamma\gamma)$  is the largest at  $m < 2m_W$ , since the  $H$  has the smallest couplings to  $gg$  and the main  $H$  decay mode in this energy region is  $b\bar{b}$ .

Concluding Remarks The measurement of the ratio [36]  $\sigma(\gamma\gamma)/\sigma(WW)$  provides a decisive way to differentiate the radion  $R$ , the dilaton  $D$ , and the SM Higgs  $H$ . It is only necessary to count the event numbers of  $\gamma\gamma$  and  $WW$  decays of an observed signal. This method is independent of the values of the model-parameters, the VEVs  $F_R$  and  $F_D$ . It applies to both the LHC and Tevatron experimental searches.

The scalars are also expected to be produced in  $W/Z$  associated production,  $W^* \rightarrow W\varphi^i$  and  $Z^* \rightarrow Z\varphi^i$ . The production cross section  $\sigma_{\text{assoc.}}(D)$  and  $\sigma_{\text{assoc.}}(R)$  are smaller than  $\sigma_{\text{assoc.}}(H)$ , respectively, by the factors  $(\frac{1}{F_D})^2$  and  $(\frac{1}{F_R})^2$ , which are  $\sim 0.01$  in the  $F_D \sim F_R \sim 3$  TeV case. This small cross section of associated production also can be used to differentiate the  $R$  and  $D$  from  $H$  [27].

The production of  $D$  and  $R$  via the  $WW, ZZ$  fusion subprocess is much smaller than that of  $H$ , due to their relatively smaller decay widths to  $WW$  and  $ZZ$ .

We may also consider the scenario that both  $D$  and  $H$  (or  $R$  and  $H$ ) exist with comparable masses in the region  $m \sim 125$  GeV, where the on-going Higgs search data show some excess over the expected SM cross section. At this mass both  $D(R)$  and  $H$  have very narrow widths,

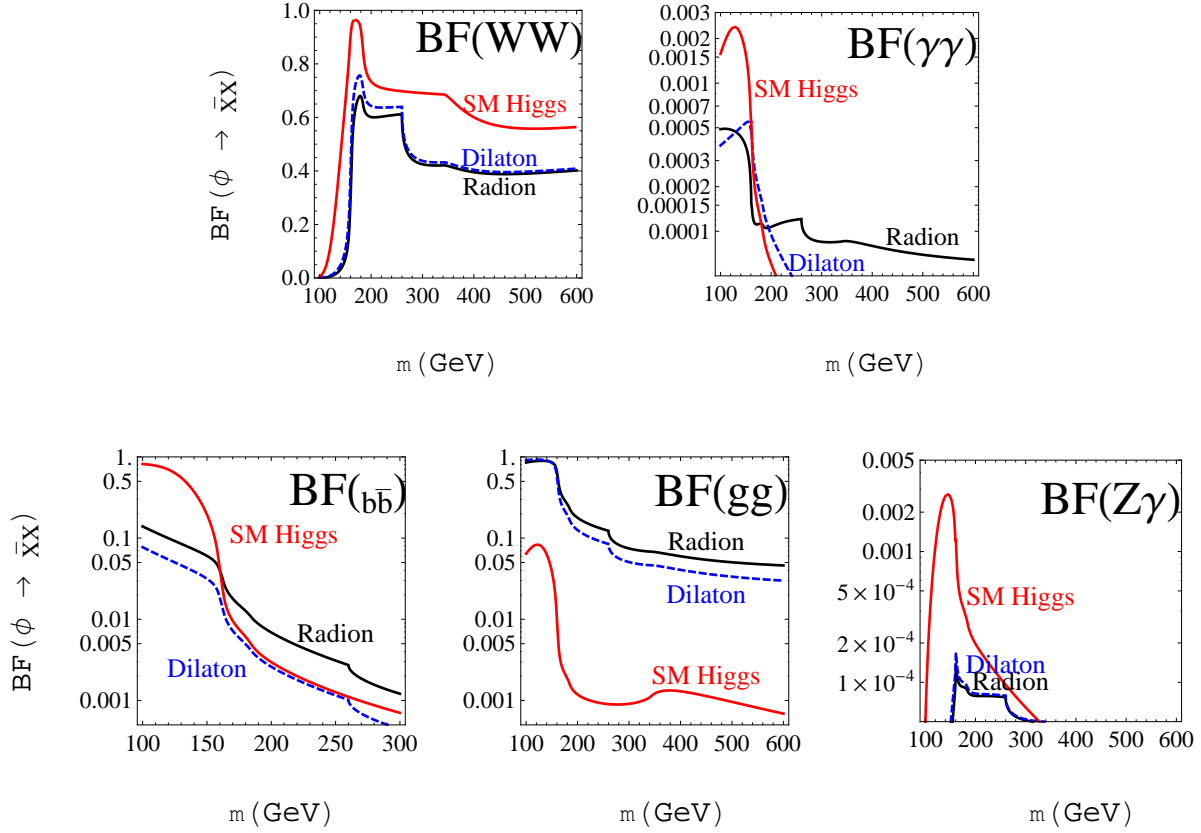


FIG. 4. Branching fractions ( $BF$ ) of the decays to  $\bar{X}X = WW, \gamma\gamma, \bar{b}b, gg, Z\gamma$ : For the radion  $R$  (black solid), the dilaton  $D$  (blue dashed), and the SM Higgs  $H$  (red dotted) in each figure. This result is independent of the model parameters,  $F_R$  for the radion and the  $F_D$  for the dilaton. For  $BF(\bar{b}b)$ ,  $I_b^R$  is taken to be 1.66 as an example.

and their resonance peaks will be smeared by experimental resolution into one with twice the production cross section, even with the mixing of scalars taken into account. In this case the  $\sigma(\gamma\gamma)/\sigma(WW)$  ratio will be intermediate between the single-state values. Another possible scenario is that  $R$  or  $D$  mix[4, 37–39] with  $H$ . Then, the lighter scalar can have a mass below 100 GeV and its production will be suppressed compared to that of the SM Higgs.

For dilaton or radion masses much larger than  $2m_W$ , the narrow width makes discovery in  $WW$  and  $ZZ$  easier than for the SM Higgs[27].

Finally, our study applies also to generic singlet models[40]. The singlet decouples from



SM particles and the phenomenology is dependent on the amount of mixing of  $H$  with the singlet scalar. The  $H$  production cross section can be significantly smaller by the mixing effect, and thus, a low-mass Higgs boson with  $m_H < 100$  GeV also become possible.

### Acknowledgements

We thank Professors Bill Bardeen and Prof. Misha Stephanov for discussions. M.I. is very grateful to the members of phenomenology institute of University of Wisconsin-Madison for hospitalities. This work was supported in part by the U.S. Department of Energy under grants No. DE-FG02-95ER40896 and DE-FG02-84ER40173, in part by KAKENHI(2274015, Grant-in-Aid for Young Scientists(B)) and in part by grant as Special Researcher of Meisei University.

- 
- [1] L. Randall and R. Sundrum, Phys. Rev. Lett. **83**, 3370 (1999).
  - [2] W. D. Goldberger, and M. B. Wise, Phys. Rev. Lett. **83**, 4922 (1999); Phys. Lett. B**475**, 275 (2000).
  - [3] Kingman Cheung, Phys. Rev. D**63**, 056007 (2001).
  - [4] G. F. Giudice, R. Rattazzi, J. D. Wells, Nucl. Phys. B**595**, 250 (2001).
  - [5] C. Csaki, J. Hubsisz, and S. J. Lee, Phys. Rev. D**76**, 125015 (2007).
  - [6] H. Davoudiasl, J. L. Hewett, and T. G. Rizzo, Phys. Lett. B**473**, 43 (2000).
  - [7] A. Pomarol, Phys. Lett. B**486**, 153 (2000).
  - [8] Y. Grossman, M. Neubert, Phys. Lett. B**474**, 361 (2000).
  - [9] T. Gherghetta, A. Pomarol, Nucl. Phys. B**586**, 141 (2000).
  - [10] K. Agashe, A. Delgado, M. J. May, and R. Sundrum, JHEP **0308**, 050 (2003).
  - [11] K. Agashe, R. Contino, and A. Pomarol, Nucl. Phys. B**719**, 165 (2005).
  - [12] C. Csaki, C. Grojean, L. Pilo, and J. Terning, Phys. Rev. Lett. **92**, 101802 (2004).
  - [13] C. Csaki, M. L. Graesser, and G. D. Kribs, Phys. Rev. D**63**, 065002 (2001).
  - [14] T. Han, G. D. Kribs, B. McElrath, Phys. Rev. D**64**, 076003 (2001).
  - [15] H. Davoudiasl, G. Perez, and A. Soni, Phys. Lett. B**665**, 67 (2008).
  - [16] H. Davoudiasl, T. McElmurry, and A. Soni, Phys. Rev. D**82**, 115028 (2010).
  - [17] M. Frank, B. Korutlu, M. Toharia, arXiv:1110.4434 [hep-ph]
  - [18] V. Barger and M. Ishida, arXiv:1110.6452[hep-ph].

- [19] W. D. Goldberger, B. Grinstein, and W. Skiba, Phys. Rev. Lett. **100**, 111802 (2008).
- [20] "Gravitation and scalar fields," Y. Fujii, Kodansha scientific 1997 (in Japanese).
- [21] K. Yamawaki, M. Bando and K. -i. Matumoto, Phys. Rev. Lett. **56**, 1335 (1986).
- [22] T. W. Appelquist, D. Karabali, and L. C. R. Wijewardhana, Phys. Rev. Lett. **57**, 957 (1986).
- [23] M. A. Luty, T. Okui, JHEP **0609**, 070 (2006).
- [24] R. Rattazzi, V. S. Rychkov, E. Tonni, A. Vichi, JHEP **0812**, 031 (2008).
- [25] D. D. Dietrich, and F. Sannino, Phys. Rev. D**72**, 055001 (2005).
- [26] V. Barger, M. Ishida, and W.-Y. Keung, arXiv:1111.2580[hep-ph].
- [27] B. Coleppa, T. Gregoire, and H. E. Logan, arXiv:1111.3276v1[hep-ph].
- [28] J. Fan, W. D. Goldberger, A. Ross, and W. Skiba, arXiv:0803.2040[hep-ph].
- [29] L. Vecchi, arXiv:1002.1721[hep-ph].
- [30] A. Azatov, M. Toharia, and L. Zhu, arXiv:0812.2489[hep-ph].
- [31] "Higgs hunters guide", J. F. Gunion, H. E. Harber, G. Kane, and S. Dawson, Perseus books 2000.
- [32] A. Djouadi, Phys.Rept. 457 (2008) 1-216.
- [33] C. Csaki, J. Erlich, and J. Terning, Phys. Rev. D**66**, 064021 (2002).
- [34] V. D. Barger and R. J. N. Phillips, "Collider Physics" Updated Edition, Westview press (1991).
- [35] S. Catani, D. de Florian, M. Grazzini, and P. Nason, JHEP**07**, 028 (2003).
- [36] I. Low and J. Lykken, JHEP 1010 (2010) 053;arXiv:1005.0872[hep-ph].
- [37] D. Dominici, B. Grzadkowski, J. F. Gunion, M. Toharia, Nucl. Phys. B**671**, 243 (2003).
- [38] M. Toharia, Phys. Rev. D**79**, 015009 (2009).
- [39] H. de Sandes and R. Rosenfeld, arXiv:1111.2006v1.
- [40] See, e.g. V. Barger, P. Langacker, and G. Shaughnessy, arXiv:10611239[hep-ph]; Phys. Rev. D**75**, 055013 (2007).